 doi:10.20944/preprints201902.0096.v1

Article

A hybrid experimental-computational approach to determine constitutive models for hyperelastic polymers

A. Karimzadeh [1], M. R. Ayatollahi [2,*], B. A. Razak [3,4], S. S. R. Koloor [5,6], M. Y. Yahya [1,*] and M. N. Tamin [5,*]

[1] Centre of Advanced Composite Materials, Universiti Teknologi Malaysia, 81310 Johor Bahru, Malaysia; a.karimzadeh.66@gmail.com, yazidyahya@utm.my
[2] Fatigue and Fracture Laboratory, Center of Excellence in Experimental Solid Mechanics and Dynamics, School of Mechanical Engineering, Iran University of Science and Technology, Tehran, 16846 Iran; m.ayat@iust.ac.ir
[3] Department of Mechanical Engineering, Faculty of Engineering, University of Malaya, 50603 Kuala Lumpur, Malaysia; bushroa@um.edu.my
[4] Centre of Advance Manufacturing and Mechanical Engineering, Faculty of Engineering, University of Malaya, 50603 Kuala Lumpur, Malaysia; bushroa@um.edu.my
[5] School of Mechanical Engineering, Universiti Teknologi Malaysia, 81310 Johor Bahru, Malaysia; s.s.r.koloor@gmail.com, nasirtamin@utm.my
[6] Department of Aerospace Engineering, Universiti Putra Malaysia, 43400 Serdang, Selangor, Malaysia; s.s.r.koloor@gmail.com
* Correspondence: m.ayat@iust.ac.ir (M.R.A.); yazidyahya@utm.my (M.Y.Y.); nasirtamin@utm.my; Tel: +60127781410 (M.N.T.)

Abstract: A study on the selection of hyperelastic constitutive model for polymeric materials is performed using a hybrid experimental-computational approach. Bis-GMA polymer is used as a case study of hyperelastic material to describe the polymer characteristics by determining its Poisson's ratio and its valid range of the hyperelastic stress-strain curves. These two parameters are then used to determine the hyperelastic constitutive model by using the hybrid approach. Several uniaxial compression tests along with their finite element simulations are implemented in a systematic way, to identify the polymer behavior under the compressive loading conditions. Nano-indentation experiments are conducted to verify the hyperelastic behavior of the polymer. The experimental and computational evidences confirm that the Poisson's ratio of Bis-GMA is 0.40 and the appropriate hyperelastic constitutive model for this polymer is of a second order polynomial. It is shown that, the results can be used to determine the true stress-strain curve of hyperelastic materials.

Keywords: hyperelastic constitutive model; Hybrid experimental-computational approach; Bis-GMA polymer; true stress-strain curve.

1. Introduction

The elastic stress-strain relation of some materials could not be described precisely by linear elastic models. Hyperelastic models are generally employed for modelling the nonlinear elastic behavior of isotropic and strain rate independent materials which behave elastically in large strains [1,2]. Identifying the appropriate constitutive models to describe the tensile and/or compressive behavior of a hyperelastic material, and defining the valid range of the hyperelastic stress-strain relation need particular considerations. A computational method based on the finite element (FE) simulation can be a powerful tool to solve this type of problems [3-5]. However, the simulation

 doi:10.20944/preprints201902.0096.v1

process requires the material nominal stress-strain curve within the range of hyperelastic response as the input data. In this respect, the knowledge of the limits of hyperelastic behavior of the material is required, which could not be determined directly and precisely from the test data. As an alternative, the mechanical behavior of hyperelastic materials can be investigated through an iterative procedure employing a hybrid experimental-computational approach. The hybrid approach normally incorporates different variables, computational models and experimental processes in an iterative procedure. As a method for solving complicated problems, the hybrid approach has been employed in the past for predicting several physical variables and mechanical properties [6,7].

Bisphenol A diglycidyl dimethacrylate or Bis-GMA polymer has many applications. For example, in dentistry, Bis-GMA is used as adhesives, sealants and base monomer of dental composite materials [8]. Bis-GMA is also employed as reinforced thermosetting plastics [9,10]. Despite extensive applications of Bis-GMA, limited information is available in the open literature about its mechanical properties. Some papers have reported the physical and mechanical properties for different combinations of Bis-GMA and other monomers such as TEGDMA [8,11]. However, very few researches have dealt with the mechanical properties of Bis-GMA alone [12]. Some mechanical properties of Bis-GMA have been measured in the past, including hardness, diametral tensile strength, flexural modulus and strength, compressive strength and Young's modulus [10,12]. In addition, in some applications of Bis-GMA where the material experiences compressive loading (such as dental restoratives and sealants), a good knowledge of compressive behavior is important while very little information is available in the literature for such conditions.

The loading-unloading response of Bis-GMA polymer needs to be examined to verify the hyperelastic behavior which has not been reported in the previous studies. On the one hand, using the uniaxial compression test to obtain the unloading behavior of polymers needs special fixtures and instruments. On the other hand, as shown in the previous studies, the loading-unloading behavior of materials within the elasticity range can be assessed by nano-indentation experiment [13-16]. Therefore, the nano-indentation tests were performed to check the elastic or the reversible behavior of the hyperelastic polymer through its loading-unloading behavior.

This study develops a hybrid approach for determination of the hyperelastic constitutive model of polymeric materials using a minimum experimental data in combination with the validated computational results. The validity and applicability of the constitutive models are examined in a case study employing the hyperelastic material, the Bis-GMA polymer. The mechanical property and behavior, in particular, the Poisson's ratio and the valid range of the stress-strain curve are determined. The results are used to obtain the true stress-strain curve of the Bis-GMA polymer. This approach is recommended for determination of the constitutive model and material behavior of different hyperelastic polymers.

2. Hybrid Experimental-Computational Aproach

The procedures used in the hybrid experimental-computational approach for determining the mechanical behavior of a hyperelastic polymer are summarized in Figure 1. At the first level, a uniaxial compression experiment is carried out. The sample preparation and the experimental procedures are described in section 3. The values of the nominal stress and nominal strain obtained from the experiment are used as the initial material properties for the finite element (FE) simulation of the compression test.

The details of the FE simulation process are explained in section 5. Since different types of hyperelasticity have been observed in the past studies, various constitutive models have also been developed and/examined for modeling the mechanical behavior of hyperelastic materials. Therefore, an appropriate constitutive model for a specific hyperelastic material should be identified through the validation of the FE simulation process and the internal analysis of the FE-calculated results, which is described in section 7 and 8, respectively. The procedure shown in Figure 1 establishes an approach to determine the constitutive model for a hyperelastic polymer and its mechanical properties, namely, the stress-strain relation and the Poisson's ratio.

Preprints (www.preprints.org) | NOT PEER-REVIEWED | Posted: 12 February 2019 doi:10.20944/preprints201902.0096.v1

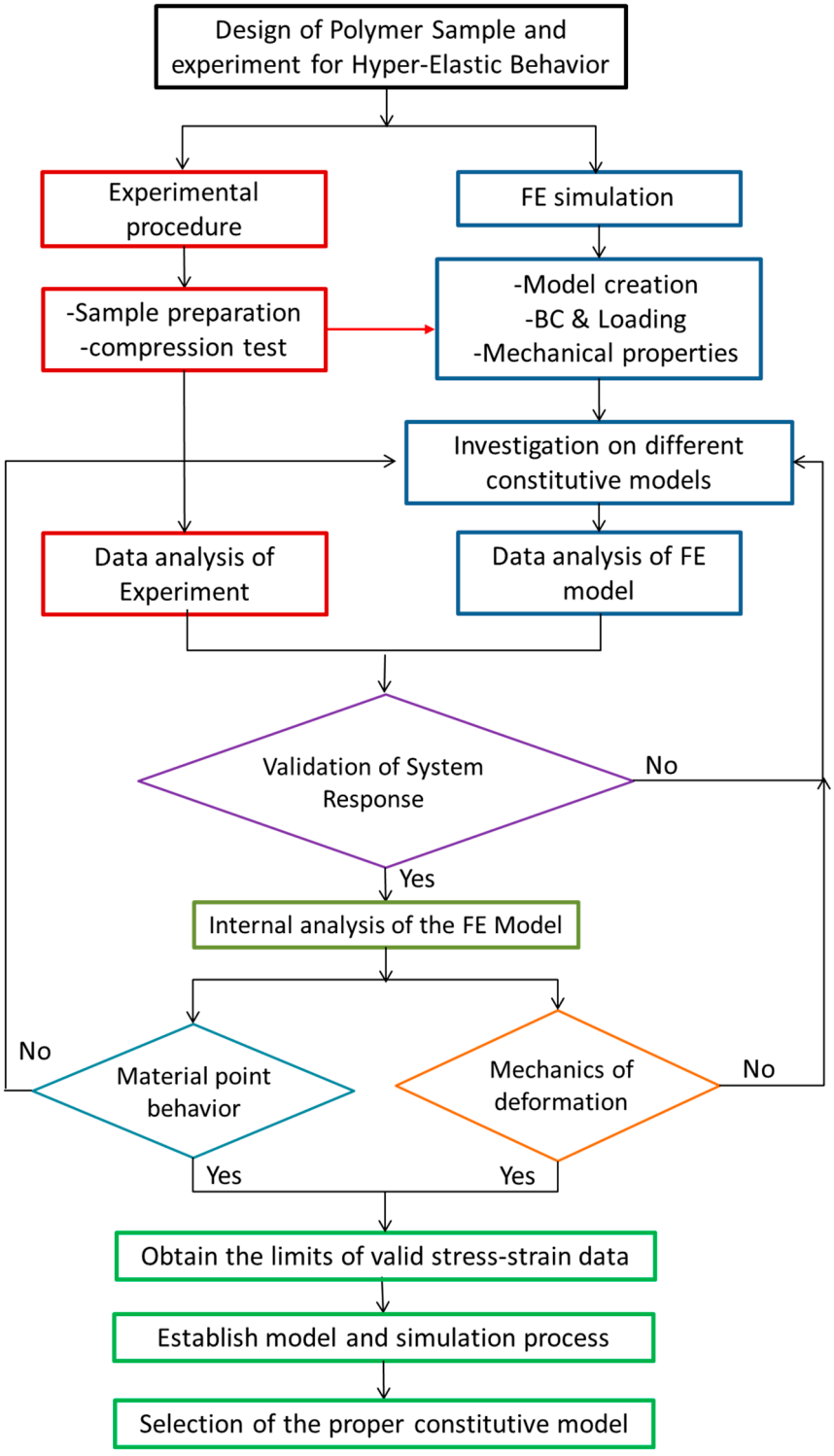

Figure 1. Flowchart of the hybrid experimental-computational approach for determining the mechanical behavior of hyperelastic polymers.

3. Materials and Methods

In this study, the Bis-GMA polymer is used as an example of hyperelastic polymers. The uniaxial compression test was performed on Bis-GMA polymer to determine its hyperelastic behavior under the compressive loading condition. The nominal stress-strain curve and the approximate maximum compressive strain at which the material behaves hyperelasticly were obtained through the experiment. In addition, the hyperelastic behavior of the polymer within the strain range that was assumed as the hyperelastic limit in compression, was examined through the loading-unloading

 doi:10.20944/preprints201902.0096.v1

curves acquired from the nano-indentation experiment. In the nano-indentation process, the material beneath the indenter tip is primarily under the compressive stress state, therefore this experiment could be used to investigate the compressive behavior of the material [17].

3.1. Sample preparation

The Bis-GMA polymer was made photo-polymerizable to form the shape of the compression test specimens by curing under a light source. For this purpose, Bis-GMA is often combined with camphoroquinone (CQ) and dimethylamine ethyl methacrylate (DMAEMA) [8,18]. The chemical characteristics of the materials used for preparing the polymer are presented in Table 1. To make a photo-polymerizable Bis-GMA, the material was heated to 50°C to reduce the viscosity for better mixing with the photo-initiators. Next, a 0.4 mol% CQ and 0.8 mol% DMAEMA were added to Bis-GMA and blended [8,18]. The mixture was stored in a dark container prior to casting.

Table 1. Chemical characteristics of the materials.

Commercial name	Chemical name	Molecular formula	Molecular weight (g/mol)	Manufacturer
Bis-GMA	2,2-bis[4-(2-hydroxy-3-methacryloxypropoxy)phenyl propane	$C_{29}H_{36}O_8$	512.59	Sigma-Aldrich Inc., St. Louis, MO, USA
Camphorquinone	2,3-bornadenione	$C_{10}H_{14}O_2$	166	Sigma-Aldrich Inc., St. Louis, MO, USA
DMAEMA	2-(dimethylamino) ethyl methacrylate	$C_7H_{14}NO_2$	157	Sigma-Aldrich Inc., St. Louis, MO, USA

Few translucent molds with a 5 mm-diameter and 11 mm-height were prepared for the compression specimens. The internal walls of the molds were lubricated thoroughly with oil for more convenient detachment of the specimen after polymerization. Then, the photo-polymerizable Bis-GMA was injected into the mold at a temperature of 50°C, and cured using a 400 W/m^2 LED light for 60 seconds from each side of the wall (i.e. top, bottom and surrounding). Next, all of the cured Bis-GMA specimens were ejected from the mold. The top and bottom surfaces of the specimens were smoothened with 400-2000 grit abrasive papers. The final height of all samples was 10±0.05 mm.

It is important to note that with elasto-plastic materials, the unloading stage of the experiments give reliable information on the elastic (thus, also on the hyperelastic) properties of the material. Therefore, a series of nano-indentation experiments were also performed to investigate the material behavior in the unloading stage of each test. The experiments were performed on a disk-shape specimen with a diameter of 5 mm and height of 4 mm, prepared using the same procedure as the compression test specimens. Since the nano-indentation experiment requires a very smooth surface, the surface of the specimen was ground with 400-2500 grit abrasive papers and polished using diamond paste with 1 and 0.5 micron-mesh sizes.

3.2. Compression test method

The uniaxial compression experiment was performed on Bis-GMA specimens with a displacement rate of 1 mm/min according to the ASTM D695 [19] standard, at room temperature using a universal testing machine (Instron, USA). The experiment was repeated for 8 specimens and the load versus load-line displacement curve was recorded for each test. Each specimen was monitored carefully during the loading to identify the approximate limit of hyperelastic behavior. It was seen that discoloration occurred in the specimen at the center and near its top and bottom surfaces. Then, some small voids like crazes were generated at the discolored area and damage could be observed visually. The machine crosshead displacement level corresponding to the observed onset

Preprints (www.preprints.org) | NOT PEER-REVIEWED | Posted: 12 February 2019 doi:10.20944/preprints201902.0096.v1

of discoloration was recorded and taken as the limit of the hyperelastic behavior. The corresponding local material displacement is determined later, through the hybrid-experimental-computational approach.

3.3. Nano-indentation test method

A series of nano-indentation experiments were carried out to examine the elastic behavior of the bis-GMA polymer through loading-unloading processes within the hyperelastic strain range, using a Triboscope test system (Hysitron Inc., USA) equipped with a Berkovich indenter. The test procedures are based on ISO 14577 [20] standard. These experiments were performed in the load-control mode with two steps of loading and unloading processes. The indenter displacement rate is 1 mm/min and the test duration is 60 seconds. The indentation load level was set to a value such that the maximum indentation strain was at the hyperelastic strain limit of up to 0.3. The indentation strain was calculated through a validated finite element simulation of nano-indentation experiment, which was performed according to the method described in a previous study [21]. However, in this study the material was considered to be hyperelastic for which the nominal stress-strain curve was obtained from the compression test and used in the finite element model.

4. Experimental results

The results of the compression and the nano-indentation experiments are presented and explained in the following sections.

4.1. Compression test results

The load versus load-line displacement curves obtained from the experiments are illustrated in Figure 2. According to the descriptions given in section 3.2, the average displacement up to which the specimens behaved hyperelastically and without any visible damage was found to be about 3 mm.

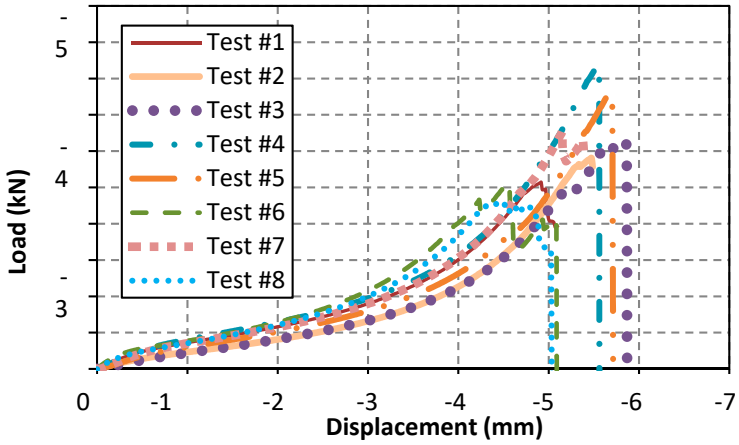

Figure 2. Load-displacement curves obtained from uni-axial compression test on Bis-GMA.

As shown in Figure 2, the load-displacement curves of the Bis-GMA specimens are close to each other up to the displacement of 3 mm. The difference between the load-displacement curves increases at displacements higher than 3 mm which can be due to the random distribution of damage within the specimens. Therefore, the compressive displacement of 3 mm can be considered as an initial estimate for the hyperelastic limit of the Bis-GMA specimens which is equal to the nominal strain of 0.3. However, more accurate hyperelastic limit of the material will be determined later, through the validation process of the FE simulation as described in section 7.

In the next stage, the values of the nominal stress and strain are calculated by dividing the force and deformation responses of the specimens (obtained from the compression test) to the original

Preprints (www.preprints.org) | NOT PEER-REVIEWED | Posted: 12 February 2019 doi:10.20944/preprints201902.0096.v1

cross-section and the original length of each specimen, respectively. Figure 3 illustrates the average stress-strain curve calculated from the experimental results. This curve is used in the next stage for defining the material behavior in the FE simulation up to the stress-strain values corresponding to the displacement of 3mm.

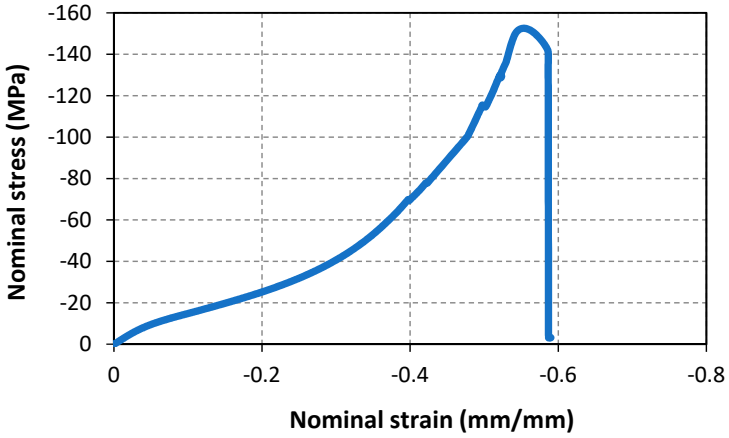

Figure 3. The mean values of nominal stress versus nominal strain obtained from the experimental results.

4.2. Nano-indentation test results

The results of nano-indentation tests were recorded as load-displacement curves as shown in Figure 4. This figure presents a sample of each load-displacement curve obtained from the experiments with two different indentation loads of 3 μN and 6 μN corresponding to the maximum indentation strains of 0.2 and 0.25, respectively. These strains are within the hyperelastic strain limit of the Bis-GMA polymer, as described earlier. The relatively higher scattered data observed in the load-displacement curve of test No. 1 (3 μN) is due to the relatively low indentation load applied to a rather soft specimen. This problem is resolved in the test No. 2 by applying a higher indentation load.

Figure 4. The loading-unloading responses of Bis-GMA in the nano-indentation test by applying an indentation load of (a) 3 μN and (b) 6 μN.

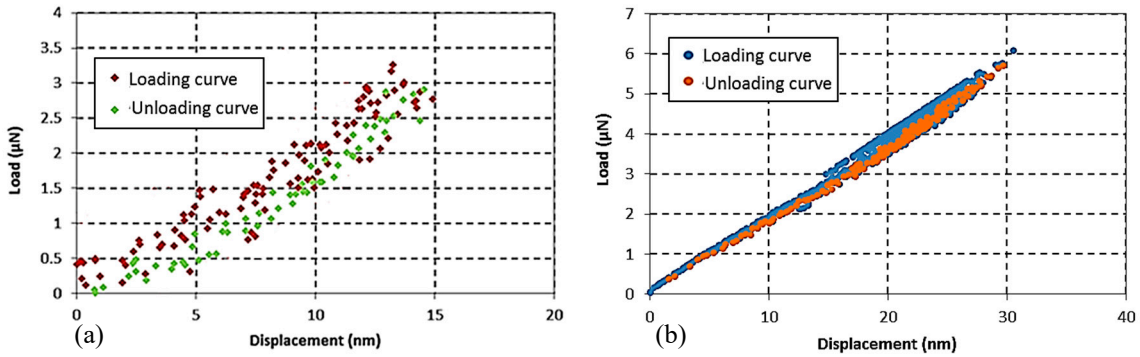

Similar traces are observed in the loading and unloading curves shown in Figure 4 indicating that the amount of plastic deformation is negligible. Moreover, the values of load reach approximately to zero at the end of the unloading process confirming the elastic behavior of the material [13,22]. The results obtained from the loading-unloading process of the nano-indentation experiment and the shape of the load-displacement curves obtained from the compression experiment confirm that the Bis-GMA polymer behaves hyperelastically under the specified compressive loading.

Preprints (www.preprints.org) | NOT PEER-REVIEWED | Posted: 12 February 2019 doi:10.20944/preprints201902.0096.v1

5. Finite element simulation

Uniaxial compression test on the polymer specimen was simulated using finite element method (FEM). A three-dimensional model was used in which a deformable cylinder for Bis-GMA specimen and two discrete rigid circular disks for the compression disks were considered, as shown in Figure 5. The non-linear geometry option was also assigned to the deformable cylindrical specimen.

The nominal stress-strain curve within the limit of hyperelastic behavior, as described in section 4.1, was used in the computational process. The Poisson's ratio is another required material parameter for the FE simulation when using uniaxial test data. For the preliminary level of the solution, the Poisson's ratio was taken as 0.45 [23-25]. This value will be refined during the validation procedure.

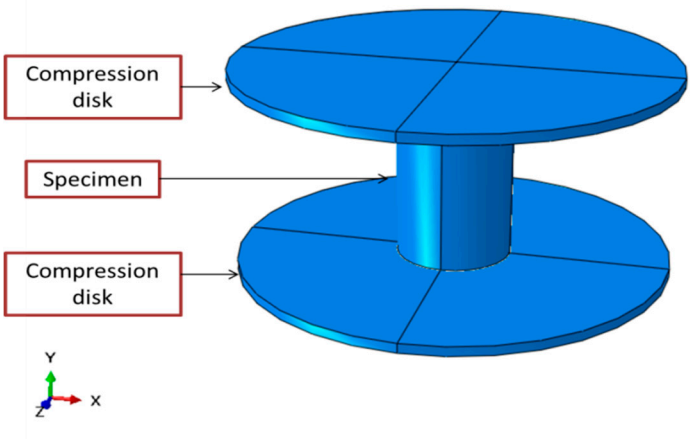

Figure 5. Geometry of FE model used for simulating the compression test.

The contact conditions between the compression disks and the test specimen were defined as a frictionless surface to surface contact with the master and the slave surfaces, respectively. The contact direction was then defined from the surface of the compression disks toward the specimen due to the fact that only the master surface can penetrate into the slave one. The finite sliding option was selected for the sliding formulation.

The boundary conditions were specified as similar to the test conditions, i.e. the lower compression disk was fixed in all directions and the upper disk was allowed to move downward along the sample axial direction. The displacement of the upper compression disk was set equal to the maximum displacement of 3 mm, which the material behaved hyperelastically. The bottom central point of the cylinder cross section was fixed the x and z directions to prevent the rigid-body motion.

The geometry of the model was meshed with 8-node linear, hybrid, constant pressure, reduced integration, hourglass control brick elements. A mesh convergence study was performed to minimize the effect of element size on the system response. The element size of the specimen was refined until the variation of the predicted load-displacement was saturated. A total number of 2200 elements were found to be sufficient for the simulation process of the compression test. These processes were performed according to the steps described in the hybrid approach, as shown in Figure 1.

6. Constitutive model

Several constitutive models have been proposed for describing the hyperelastic material behavior. The experimental stress-strain curves can be used in a comparative method to determine the most appropriate model for a specific material. A list of hyperelastic models that are used in the present study is shown in Table 2.

In the constitutive equations mentioned in Table 2, U is the strain energy per unit of reference volume or the strain energy density, C, D, μ and λ_m are material parameters, J^{el} is the elastic volume

Preprints (www.preprints.org) | NOT PEER-REVIEWED | Posted: 12 February 2019 doi:10.20944/preprints201902.0096.v1

ratio, $\bar{I}_1$ and $\bar{I}_2$ are the first and second deviatoric strain invariants which, with the assumption of full incompressibility for the material, are defined as:

$$J^{el} = (\lambda_1\lambda_2\lambda_3)^{el} = 1 \quad (1)$$

$$\bar{I}_1 = \lambda_1^2 + \lambda_2^2 + \lambda_3^2 \quad (2)$$

$$\bar{I}_2 = \lambda_1^{(-2)} + \lambda_2^{(-2)} + \lambda_3^{(-2)} \quad (3)$$

where λ_1, λ_2 and λ_3 are the principal stretches and the superscript *el* refers to the elastic limit. Detailed information about the equations and models could be found in the references given in the left column of Table 2.

Table 2. Several hyperelastic models suggested for the polymer materials.

Model name	Constitutive equation	Detail
Arruda-Boyce form [26]	$U = \mu\left\{\frac{1}{2}(\bar{I}_1 - 3) + \frac{1}{20\lambda_m^2}(\bar{I}_1^2 - 9) + \frac{11}{1050\lambda_m^4}(\bar{I}_1^3 - 27) + \frac{19}{7000\lambda_m^6}(\bar{I}_1^4 - 81) + \frac{519}{673750\lambda_m^8}(\bar{I}_1^5 - 243)\right\} + \frac{1}{D}\left(\frac{J_{e\ell}^2 - 1}{2} - \ln J_{e\ell}\right)$	-
Polynomial form [27]	$U = \sum_{i+j=1}^{N} C_{ij}(\bar{I}_1 - 3)^i(\bar{I}_2 - 3)^j + \sum_{i=1}^{N}\frac{1}{D_i}(J^{e\ell} - 1)^{2i}$	N=1, 2
Reduced polynomial form [28]	$U = \sum_{i=1}^{N} C_{i0}(\bar{I}_1 - 3)^i + \sum_{i=1}^{N}\frac{1}{D_i}(J^{e\ell} - 1)^{2i}$	N=1, 2,…, 6
Ogden form [29]	$U = \sum_{i=1}^{N}\frac{2\mu_i}{\alpha_i^2}(\bar{\lambda}_1^{\alpha_i} + \bar{\lambda}_2^{\alpha_i} + \bar{\lambda}_3^{\alpha_i} - 3) + \sum_{i=1}^{N}\frac{1}{D_i}(J^{e\ell} - 1)^{2i}$	N=1, 2,…, 6
Yeoh form [30]	$U = C_{10}(\bar{I}_1 - 3) + C_{20}(\bar{I}_1 - 3)^2 + C_{30}(\bar{I}_1 - 3)^3 + \frac{1}{D_1}(J^{e\ell} - 1)^2 + \frac{1}{D_2}(J^{e\ell} - 1)^4 + \frac{1}{D_3}(J^{e\ell} - 1)^6$	Reduced polynomial N=3
Van der Waals form [31]	$U = \mu\left\{-(\lambda_m^2 - 3)\left[\ln(1-\eta) + \eta\right] - \frac{2}{3}a\left(\frac{\tilde{I} - 3}{2}\right)^{\frac{3}{2}}\right\} + \frac{1}{D}\left(\frac{J_{e\ell}^2 - 1}{2} - \ln J_{e\ell}\right)$	-

The suitable constitutive model for representing the hyperelastic behavior of the tested material is initially unknown. Therefore, in the first step of the FE simulation, the hyperelastic response of each model of the tested polymer was evaluated by simulating a single continuum element of the Bis-GMA polymer with unit dimensions under uniaxial compression. The unknown parameters of the hyperelastic models were obtained in a curve fitting process using the uniaxial compression test data. Since the number of equations is greater than the number of unknown constants, a least-squared fitting method should be used. In the least-squared curve fitting method the following error function *E* is minimized for the '*n*' number of stress and strain pair points that are obtained from the test data. The function is given as:

$$E = \sum_{i=1}^{n}(1 - \frac{T_i^{th}}{T_i^{test}})^2 \quad (4)$$

where T_i^{th} is the theoretical stress expression related to the constitutive models and T_i^{test} is a stress value obtained from the experimental data. In the uniaxial tests, the theoretical stress (T^{th}) can be calculated from the uniaxial stress (T_u) which is derived from the strain energy density by applying the principle of virtual work as follows:

Preprints (www.preprints.org) | NOT PEER-REVIEWED | Posted: 12 February 2019 doi:10.20944/preprints201902.0096.v1

$$T_u = \frac{\delta U}{\delta \lambda_u} \quad (5)$$

where λ_u is the stretch in the loading direction.

Figure 6 displays the stress–strain results of the hyperelastic models obtained from the single element simulation in comparison with the test data. As shown in the figure, the results of the second order polynomial (i.e. polynomial N=2), Van der Waals and Yeoh models are relatively close to the stress-strain curve obtained from the experiment. Therefore, these three hyperelastic models can be considered as suitable models for the simulation of Bis-GMA polymer behavior. In the next step, the most appropriate model among these three models is determined through the iterative procedure, as shown in the flowchart in Figure 1.

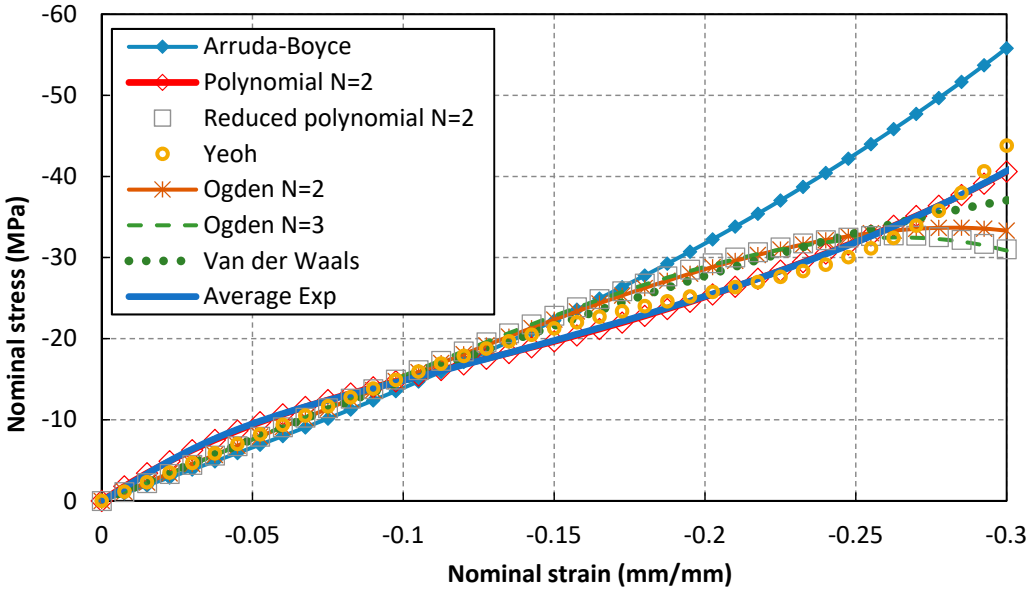

Figure 6. The resulting stress-strain curves that were fitted using the hyperelastic models provided in Table 2.

7. Validation of the FE simulation

The validation process is a procedure that investigates the accuracy of the simulation process. In this procedure, the predicted system response of the FE model is compared with the test data. The force applied by the compression disks to the specimen versus the displacement of the upper disk is considered as the system response in the validation procedure.

According to the flowchart shown in Figure 1, in the validation procedure, the constitutive model, the Poisson's ratio and the valid range of the nominal stress-strain curve for the hyperelastic behavior of the sample material are the variables that could be changed in each iteration. Moreover, the approximate validity limit of the nominal stress-strain curve for hyperelastic behavior and the maximum possible value of the Poisson's ratio of the material are determined, as described in detail in sections 4 to 6.

To obtain the abovementioned variables, in the first stage the Poisson's ratio of the sample material was determined for all the three selected hyperelastic models (i.e. polynomial N=2, Van der Waals and Yeoh models). For this purpose, the value of the Poisson's ratio was reduced from the maximum of 0.45, as proposed in [23-25] through the iterative FE simulation process. At the end of each iteration, the load-displacement curve obtained from the FE simulation was compared with the average experimental load-displacement curve. This process was repeated until no significant difference was observed in the results of the FE simulation. By using this method, the Poisson's ratio of Bis-GMA was obtained as 0.40 which was then used in the rest of FE simulations. It is useful to note that the obtained value of Poisson's ratio is in the range for the common polymer materials.

In the second stage of the validation process, the validity limit of the stress-strain curves for the hyperelastic models was specified. As mentioned earlier, the system response for hyperelastic

Preprints (www.preprints.org) | NOT PEER-REVIEWED | Posted: 12 February 2019 doi:10.20944/preprints201902.0096.v1

behavior is valid up to the point where no visible physical damage is observed. The system response was defined earlier as the load applied by the compression disks to the specimen versus the displacement of the disks. The load-displacement responses of the polymer predicted using the selected hyperelastic models are compared with the experimental data, as shown in Figure 7.

Figure 7 indicates that the maximum difference between the FE simulation and the experimental results in the polynomial N=2 is less than those of the Van der Waals and Yeoh models. A similar trend is observed between the system responses predicted by the FE simulation and the experimental data for all the models within the limit of 0 to 2.5 mm compressive displacement as illustrated in Figure 7, while considerable dissimilarity is seen beyond that range. Therefore, the maximum value of the displacement due to the hyperelastic material behavior was deduced to be about 2.5 mm when using the polynomial, Van der Waals and Yeoh hyperelastic models in the FE simulation. At this displacement, the maximum difference between the load obtained from the simulation and the average value measured from the experiments is less than 30%.

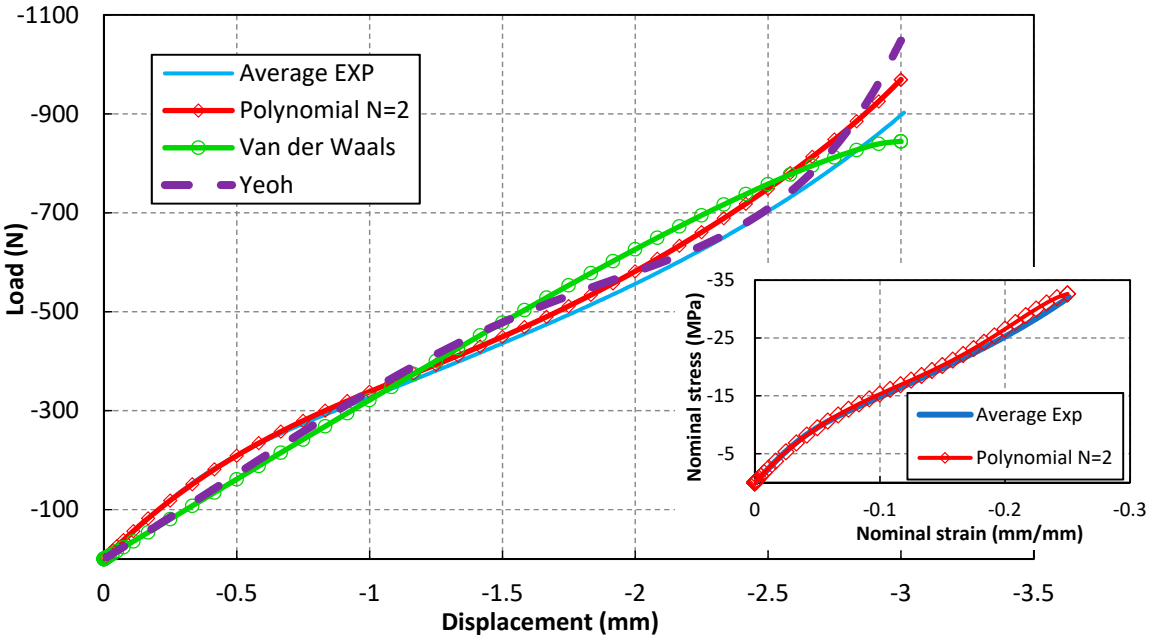

Figure 7. The predicted load-displacement curves and stress-strain responses of the system in comparison with the experimental data.

In the next step, the appropriate constitutive model is chosen through the internal analysis of the FE models by studying the mechanics of deformation as well as the stress-strain relation.

8. Internal analysis of the FE model

Internal analysis is a process that investigates the local material behavior, i.e. the variations of stress or strain parameters in material points (or nodes in the FE simulation). It also studies the integration of the local material behavior to form the structural response as the overall deformation of the structure. The internal analysis is considered as the second stage of the hybrid approach after the validation process for selection of the constitutive model, as described in the next sections.

8.1. Analysis of the mechanics of deformation

Analysis of the mechanics of deformation is a process in which the predicted geometry of the loaded specimen obtained from the FE simulation is compared with the corresponding specimen in the experimental counterpart. The predicted results show that applying different hyperelastic equations in the FE simulation affects the calculated deformation, thus the shape of the specimen. It is inferred that the input data for the hyperelastic models which is the nominal stress-strain curve and the Poisson's ratio have significant influence on the load-displacement curve obtained from the

Preprints (www.preprints.org) | NOT PEER-REVIEWED | Posted: 12 February 2019 doi:10.20944/preprints201902.0096.v1

FE simulation, as assessed in the validation process. Therefore, hyperelastic equations applied in the FE simulation should be changed through the iterations employed in the analysis of the mechanics of deformation according to the flowchart shown in Figure 1, in order to choose the constitutive model of the polymer. Figure 8 shows a cut-out half view of the specimen illustrating the transverse deformation to the loading direction. The selected equations (i.e. polynomial N=2, Van der Waals and Yeoh) were used in the computational process and the images were captured at 2.5 mm compressive displacement as the limit of the hyperelastic behavior of Bis-GMA polymer.

The expansions of the cross-sectional area of the cylinder are determined for various hyperelastic equations along the sample height (see Figure 8). In the case where Yeoh model is applied, the maximum diameter expansion of 0.74 mm was obtained which is less than the corresponding value measured in the experiments (0.8-1 mm). The maximum diameter expansion of 0.88 and 0.86 mm is obtained using the Van der Waals and polynomial N=2 model, respectively, which are in the range of experiment (0.8-1 mm). According to the physical deformation of the sample during the test (Figure 9), the diameter of the central section of the specimen is slightly more than the top and bottom surfaces which is also predicted in the FE simulation using the polynomial N=2 and Van der Waals models. A better sense to such deformations could be seen by monitoring the diameter variation through an axial path, as shown in Figure 10.

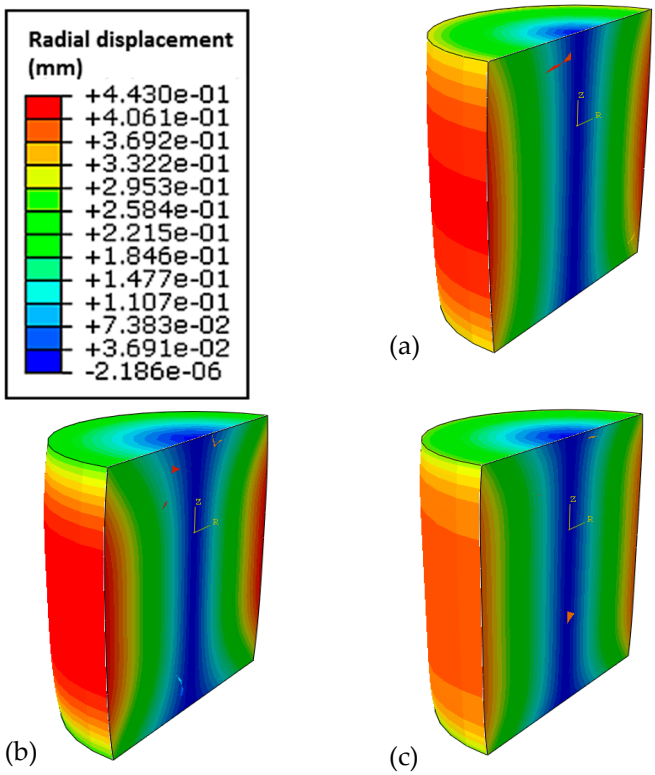

Figure 8. Contour plots of the specimen radial deformation computed using (a) polynomial N=2, (b) Van der Waals and (c) Yeoh models.

This process confirms that the simulation of the sample material using the polynomial N=2 and Van der Waals models could provide good predictions for the mechanics of structural deformation in Bis-GMA polymer. However, further investigation is performed in the next section by studying the stress-strain curve of the polymer using the same models (i.e. polynomial N=2, Van der Waals and Yeoh).

Preprints (www.preprints.org) | NOT PEER-REVIEWED | Posted: 12 February 2019 doi:10.20944/preprints201902.0096.v1

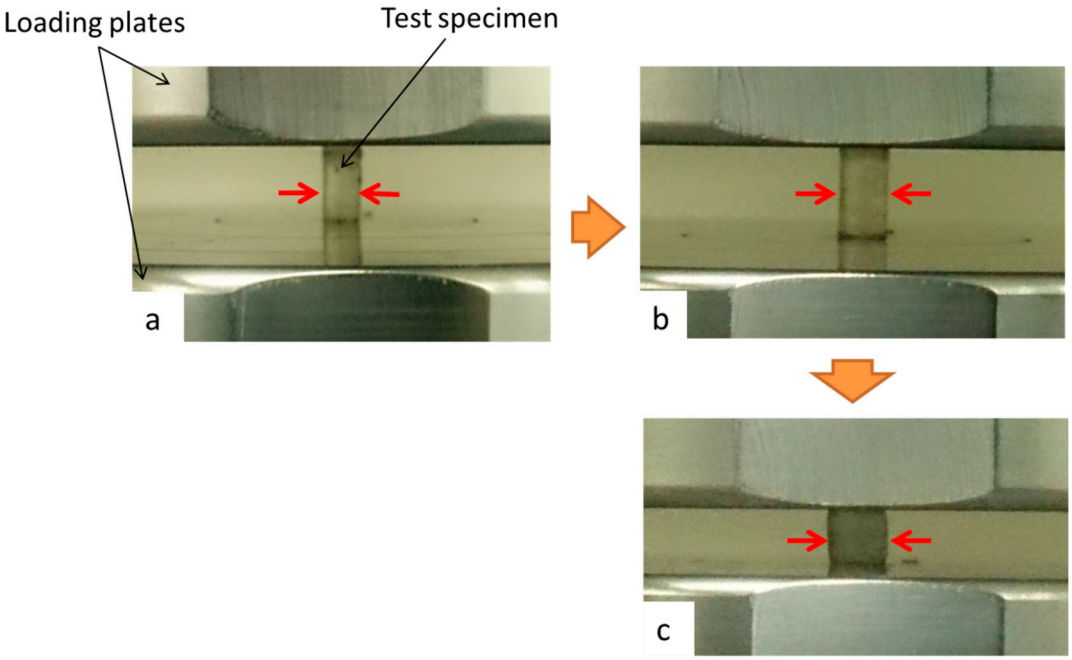

374

375 **Figure 9.** Deformation of the specimen, (a) before loading, (b) at the middle and (c) at the end of the
376 hyperelastic behavior limit.

377

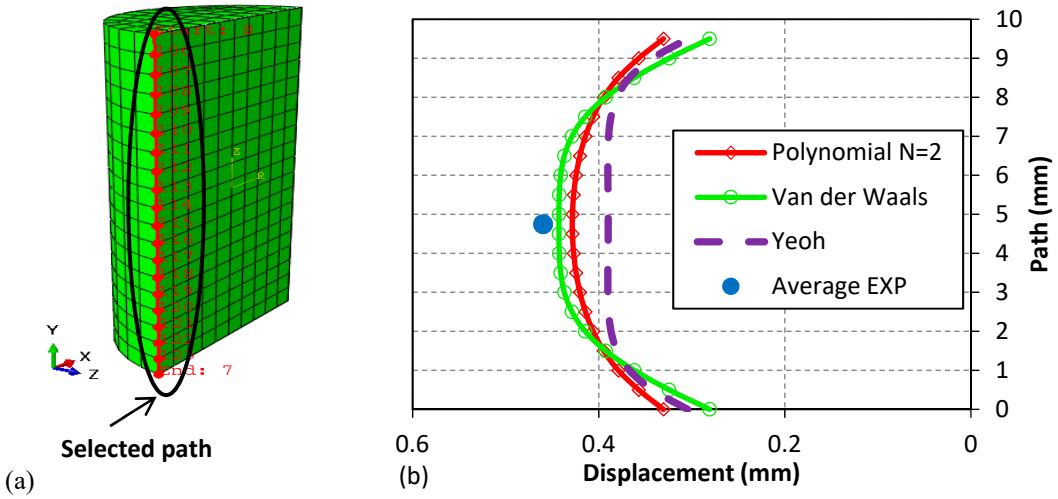

378 **Figure 10.** Deformation of the sample (a) selected axial path on the cylinder, (b) the variation of
379 diameter expansion along the cylinder height.

380 *8.2. Analysis of the stress-strain curve*

381 In this section, the structural response of the specimen is assessed using the true stress-true strain
382 curve. Since considering any of the hyperelastic models could result in different structural
383 deformations, the examination of the true stress-strain curve could provide a better insight into the
384 selection of the constitutive models. Therefore, the true stress-strain curve of the material together
385 with the corresponding experimental curve is obtained and plotted in Figure 11. The true stress-strain
386 values for each hyperelastic model were obtained based on the computed load response of the
387 specimen, while the variations of the cross-section were recorded during the loading in the FE
388 simulation.

Preprints (www.preprints.org) | NOT PEER-REVIEWED | Posted: 12 February 2019 doi:10.20944/preprints201902.0096.v1

The results indicate that the data provided from the polynomial N=2 model is in a better agreement with the experimental results, in comparison with the results of the Van der Waals and Yeoh models. The FE results of the polynomial N=2 predict the experimental curve of the polymer precisely up to the 0.1mm/mm compressive strain, but overestimate the test results slightly for larger strains. This could be due to the associated uncertainty in measuring the cross-sectional area of the specimen during the experiment. In addition, the likely presence of defects in the samples and the measurement errors during the experimental process (which are not considered in the FE model) could cause the observed discrepancy. Meanwhile, a 6% error in the prediction of the true stress at 0.2 mm/mm strain is considered as acceptable.

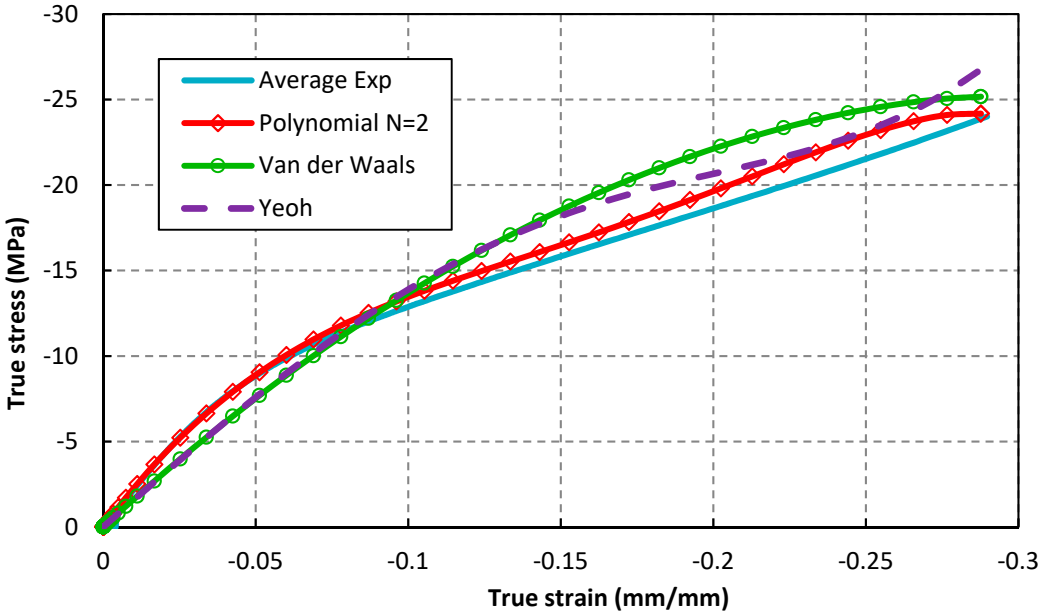

Figure 11. The true stress-strain curves obtained from the structural response of the model using different hyperelastic equations.

The results of the present study, which were obtained through the validation and internal analysis processes in the hybrid experimental-computational approach, confirm the selection of the second order polynomial model (i.e. polynomial N=2) as the best model for the description of the hyperelastic behavior of Bis-GMA polymer. The constitutive equation of the polynomial N=2 model can be obtained by expanding the general polynomial form equation [27] in Table 2 for N=2 which gives:

$$U = C_{01}(\bar{I}_2 - 3) + C_{10}(\bar{I}_1 - 3) + C_{11}(\bar{I}_1 - 3)(\bar{I}_2 - 3) + C_{02}(\bar{I}_2 - 3)^2 + C_{20}(\bar{I}_1 - 3)^2 + D_1^{(-1)}(J^{el} - 1)^2 + D_2^{(-1)}(J^{el} - 1)^4 \quad (6)$$

where U is the strain energy per unit of reference volume. The parameters J, $\bar{I}_1$ and $\bar{I}_2$ (presented in Eqs (1) to (3)) are calculated for the uniaxial compressive behavior of a single element up to the displacement of 2.5 mm. In Eq. (6), C and D are material constants which are calculated by a curve fitting process, as described in section 6. These material constants were determined in this study for Bis-GMA as:

$C_{01} = -259.62MPa$, $C_{10} = 300.35MPa$, $C_{11} = 279.21MPa$, $C_{02} = -187.68MPa$, $C_{20} = 81.33MPa$, $D_1 = 0MPa^{-1}$, $D_2 = 0MPa^{-1}$.

As mentioned earlier, Bis-GMA is frequently used as a matrix phase for dental composite restoratives and adhesives [8,12,32]. However, to interpret the mechanical behavior of the composites, better understanding of the matrix behavior is necessary [33-35]. Since Bis-GMA is known to be a hyperelastic polymer, the assumption of a linear stress-strain relation cannot accurately describe its real mechanical behavior. Meanwhile, the hyperelastic material properties of Bis-GMA have not been reported in the literature. This could be due to the lack of a standard or a

straightforward method on how to determine these material parameters. This study have introduced and developed a hybrid experimental-computational approach for determining the hyperelastic mechanical parameters of polymeric materials with particular emphasis on the Bis-GMA polymer.

9. Conclusion

An investigation was performed on the hyperelastic constitutive models for polymeric materials using a hybrid experimental-computational approach. Bis-GMA polymer was used as the case study of hyperelastic materials. Several uniaxial compression experiments were performed to determine the Bis-GMA nominal stress-strain curve and estimate the strain limit of the hyperelasitc behavior. The hyperelastic behavior of the material was also confirmed through loading-unloading curves obtained from the nano-indentation experiments in combination with the compression test. The hybrid experimental-computational approach was applied to Bis-GMA polymer to obtain its constitutive model and mechanical characteristics under compressive loading conditions, including the valid range of the nominal stress-strain curve for hyperelastic behavior and the Poisson's ratio. Results showed that the maximum nominal strain value in which the material behaves hyperelastically was equal to 0.25 mm/mm and the Poisson's ratio of Bis-GMA was obtained as 0.40. Moreover, the second order polynomial was selected for the hyperelastic constitutive model of Bis-GMA polymer. It was shown that the results can be accurately used to obtain the true stress-strain curve of hyperelastic materials. The hybrid approach presented in this paper can be recommended for determining the constitutive models of polymeric materials that exhibit hyperelastic behavior.

Author Contributions: Conceptualization, Atefe Karimzadeh, Majid R Ayatollahi and Seyed S R Koloor; Data curation, Atefe Karimzadeh; Formal analysis, Atefe Karimzadeh; Funding acquisition, Bushroa A Razak , Mohd Y Yahya and Mohd N Tamin; Investigation, Atefe Karimzadeh, Majid R Ayatollahi and Mohd N Tamin; Methodology, Atefe Karimzadeh and Seyed S R Koloor; Project administration, Atefe Karimzadeh and Bushroa A Razak ; Resources, Bushroa A Razak , Mohd Y Yahya and Mohd N Tamin; Software, Atefe Karimzadeh and Seyed S R Koloor; Supervision, Majid R Ayatollahi and Mohd Y Yahya; Validation, Majid R Ayatollahi, Seyed S R Koloor and Mohd N Tamin; Visualization, Atefe Karimzadeh; Writing – original draft, Atefe Karimzadeh and Seyed S R Koloor; Writing – review & editing, Majid R Ayatollahi, Bushroa A Razak and Mohd N Tamin.

Funding: This research received no external funding rather than those mentioned in the Acknowledgments.

Acknowledgments: Dr. Atefeh Karimzadeharani is a researcher of UTM under the Postdoctoral Fellowship Scheme for the project: "Development of Soft Composite Materials with Improved Impact Resistance Using Natural Fabric and Nano-Silica Based Shear Thickening Fluid (STF)". The authors would like to acknowledge the Ministry of Higher Education, Malaysia for providing a high impact research (HIR) grant with number UM.C/625/1/HIR/MOHE/ENG/27. This research is also partly funded under the University of Malaya under UMRG programme grant number of UM.TNC2/RC/AET/261/1/1/RP017-2012C, and Universiti Teknologi Malaysia under Matching Grant No. 01M01.

Conflicts of Interest: The authors declare no conflict of interest.

References

1. Basar, Y.; Weichert, D. Nonlinear continuum mechanics of solids, Chapter 6: Constitutive modelling; Springer: Germany, 2000.
2. Muhr, A.H. Modeling the Stress-Strain Behavior of Rubber. Rubber Chemistry and Technology 2005, 78, 391-425, doi:10.5254/1.3547890.
3. Khajehsaeid, H.; Arghavani, J.; Naghdabadi, R.; Sohrabpour, S. A visco-hyperelastic constitutive model for rubber-like materials: A rate-dependent relaxation time scheme. Int J Eng Sci 2014, 79, 44-58, doi:http://dx.doi.org/10.1016/j.ijengsci.2014.03.001.
4. Yang, L.M.; Shim, V.P.W.; Lim, C.T. A visco-hyperelastic approach to modelling the constitutive behaviour of rubber. Int J Impact Eng 2000, 24, 545-560, doi:http://dx.doi.org/10.1016/S0734-743X(99)00044-5.
5. Chen, Z.W.; Joli, P.; Feng, Z.Q. Anisotropic hyperelastic behavior of soft biological tissues. Comput Method Biomec 2015, 18, 1436-1444, doi:10.1080/10255842.2014.915082.

6. Meredig, B.; Wolverton, C. A hybrid computational–experimental approach for automated crystal structure solution. Nat Mater 2013, 12, 123-127, doi:http://www.nature.com/nmat/journal/v12/n2/abs/nmat3490.html#supplementary-information.
7. Tamin, M.N.; Nor, F.M.; Wei Keat, L. Hybrid Experimental-Computational Approach for Solder/IMC Interface Shear Strength Determination in Solder Joints. IEEE Transaction on Components and Packaging Techologies 2010, 33(3), 614-620, doi:10.1109/TCAPT.2010.2050887.
8. Gajewski, V.; Pfeifer, C.; Fróes-Salgado, N.; Boaro, L.; Braga, R. Monomers Used in Resin Composites: Degree of Conversion, Mechanical Properties and Water Sorption/Solubility. Braz Dent J. 2012, 23, 508-514.
9. Yilgör, I.; Yilgör, E.; Banthia, A.K.; Wilkes, G.L.; McGrath, J.E. Synthesis and characterization of free radical cured Bis-methacryloxy bisphenol-A epoxy networks. Polym Composite 1983, 4, 120-125, doi:10.1002/pc.750040207.
10. Praharaj, A.P.; Behera, D.; Bastia, T.K. Fabrication and Mechanical Properties of BisGMA/Amine Functionalized Paper Pulp Composites International Journal of Innovative Research in Science, Engineering and Technology 2014, 3, 12719-12723.
11. Tiwari, A.; Polykarpov, A. Photocured Materials, Volume 13 of Rsc Smart Materials, Chapter 15: Methacrylate and Epoxy Resins Photocured by Means of Visible Light-Emitting Diodes (LEDs); Royal Society of Chemistry: UK, 2014; pp. 370.
12. Emami, N.; Soderholm, K. Young's modulus and degree of conversion of different combination of light-cure dental resins. The open dentistry journal 2009, 3, 202-207, doi:10.2174/1874210600903010202.
13. Chen, Z.; Diebels, S. Modelling and parameter re-identification of nanoindentation of soft polymers taking into account effects of surface roughness. Computers & Mathematics with Applications 2012, 64, 2775-2786, doi:http://dx.doi.org/10.1016/j.camwa.2012.04.010.
14. Luczynski, K.W.; Dejaco, A.; Lahayne, O.; Jaroszewicz, J.; W.Swieszkowski; Hellmich, C. MicroCT/Micromechanics-Based Finite Element Models and Quasi-Static Unloading Tests Deliver Consistent Values for Young's Modulus of Rapid-Prototyped Polymer-Ceramic Tissue Engineering Scaffold. 2012.
15. Lin, D.C.; Shreiber, D.I.; Dimitriadis, E.K.; Horkay, F. Spherical indentation of soft matter beyond the Hertzian regime: numerical and experimental validation of hyperelastic models. Biomechanics and modeling in mechanobiology 2009, 8, 345-358, doi:10.1007/s10237-008-0139-9.
16. Mathews, M.; Wang, H.-T.; Li, L. Finite Element Analysis of Nanoindentation and Elastic Behavior of Bi2Te3 Two-Dimensional Nanosheets. ECS Journal of Solid State Science and Technology 2016, 5, Q3082-Q3087.
17. Mishra, M.; Szlufarska, I. Possibility of high-pressure transformation during nanoindentation of SiC. Acta Materialia 2009, 57, 6156-6165, doi:http://dx.doi.org/10.1016/j.actamat.2009.08.041.
18. Randolph, L.D.; Palin, W.M.; Bebelman, S.; Devaux, J.; Gallez, B.; Leloup, G.; Leprince, J.G. Ultra-fast light-curing resin composite with increased conversion and reduced monomer elution. Dental Materials 2014, 30, 594-604, doi:10.1016/j.dental.2014.02.023.
19. ASTM D695-15. In Standard Test Method for Compressive Properties of Rigid Plastics, ASTM International: West Conshohocken, PA 19428-2959. United States, 2015.
20. ISO-14577-1. Metallic Materials — Instrumented Indentation Test for Hardness and Materials Parameters In Part 1: Test Method, Geneva: Switzerland, 2002.
21. Karimzadeh, A.; Ayatollahi, M.R.; Alizadeh, M. Finite element simulation of nano-indentation experiment on aluminum 1100. Computational Materials Science 2014, 81, 595-600, doi:http://dx.doi.org/10.1016/j.commatsci.2013.09.019.
22. Oliver, W.C.; Pharr, G.M. Measurement of hardness and elastic modulus by instrumented indentation: Advances in understanding and refinements to methodology. J. Mater. Res. 2004, 19, 3-20.
23. Greaves, G.N.; Greer, A.L.; Lakes, R.S.; Rouxel, T. Poisson's ratio and modern materials. Nat Mater 2011, 10, 823-837.
24. Mott, P.H.; Roland, C.M. Limits to Poisson's ratio in isotropic materials. Phys Rev B 2009, 80, 132104-132108.
25. Chapter 5: Poisson's Ratio and Mechanical Nonlinearity Under Tensile Deformation in Crystalline Polymers. Nitta, K.-h.; Yamana, M., Eds.; InTech: Croatia 2012; p 113-130.
26. Arruda, E.M.; Boyce, M.C. A three-dimensional constitutive model for the large stretch behavior of rubber elastic materials. J Mech Phys Solids 1993, 41, 389-412, doi:http://dx.doi.org/10.1016/0022-5096(93)90013-6.

27. Bower, A.F. Applied Mechanics of Solids, Chapter 3: Constitutive Equations: Relations between Stress and Strain; CRC Press: 2009.
28. Abaqus 6.14 Online Documentation, Section 22.5.1 of the Abaqus Analysis User's Guide: Hyperelastic behavior of rubberlike materials, . Dassault Systèmes, Ed. 2014.
29. Ogden, R.W. Large Deformation Isotropic Elasticity - On the Correlation of Theory and Experiment for Incompressible Rubberlike Solids. Proceedings of the Royal Society of London. A. Mathematical and Physical Sciences 1972, 326, 565-584.
30. Yeoh, O.H. Characterization of Elastic Properties of Carbon-Black-Filled Rubber Vulcanizates. Rubber Chem Technol 1990, 63, 792-805, doi:doi:10.5254/1.3538289.
31. Kilian, H.G.; Enderle, H.F.; Unseld, K. The use of the van der Waals model to elucidate universal aspects of structure-property relationships in simply extended dry and swollen rubbers. Colloid Polym Sci 1986, 264, 866-876, doi:10.1007/BF01410637.
32. Walsh, W.R.; Svehla, M.J.; Russell, J.; Saito, M.; Nakashima, T.; Gillies, R.M.; Bruce, W.; Hori, R. Cemented fixation with PMMA or Bis-GMA resin hydroxyapatite cement: effect of implant surface roughness. Biomaterials 2004, 25, 4929-4934, doi:http://dx.doi.org/10.1016/j.biomaterials.2003.12.020.
33. Hua, Y.; Gu, L.; Watanabe, H. Micromechanical analysis of nanoparticle-reinforced dental composites. Int J Eng Sci 2013, 69, 69-76, doi:http://dx.doi.org/10.1016/j.ijengsci.2013.04.001.
34. Sideridou, I.; Tserki, V.; Papanastasiou, G. Effect of chemical structure on degree of conversion in light-cured dimethacrylate-based dental resins. Biomaterials 2002, 23, 1819-1829, doi:http://dx.doi.org/10.1016/S0142-9612(01)00308-8.
35. Venter, S.A.d.S.; Fávaro, S.L.; Radovanovic, E.; Girotto, E.M. Hardness and degree of conversion of dental restorative composites based on an organic-inorganic hybrid. Mat Res 2013, 16, 898-902.